Nanoscale Res Lett (2010) 5:1692–1697
DOI 10.1007/s11671-010-9698-7

NANO EXPRESS

Growth of Inclined GaAs Nanowires by Molecular Beam Epitaxy: Theory and Experiment

X. Zhang · V. G. Dubrovskii · N. V. Sibirev · G. E. Cirlin · C. Sartel · M. Tchernycheva · J. C. Harmand · F. Glas

Received: 2 June 2010 / Accepted: 2 July 2010 / Published online: 24 July 2010

Abstract The growth of inclined GaAs nanowires (NWs) during molecular beam epitaxy (MBE) on the rotating substrates is studied. The growth model provides explicitly the NW length as a function of radius, supersaturations, diffusion lengths and the tilt angle. Growth experiments are carried out on the GaAs(211)A and GaAs(111)B substrates. It is found that 20° inclined NWs are two times longer in average, which is explained by a larger impingement rate on their sidewalls. We find that the effective diffusion length at 550°C amounts to 12 nm for the surface adatoms and is more than 5,000 nm for the sidewall adatoms. Supersaturations of surface and sidewall adatoms are also estimated. The obtained results show the importance of sidewall adatoms in the MBE growth of NWs, neglected in a number of earlier studies.

Keywords Inclined GaAs nanowires · Molecular beam epitaxy · Surface diffusion

X. Zhang
Key Laboratory of Information Photonics and Optical Communications (Ministry of Education), Beijing University of Posts and Telecommunications, P.O. Box 66, 100876 Beijing, China

X. Zhang · V. G. Dubrovskii · N. V. Sibirev · G. E. Cirlin
St.-Petersburg Academic University RAS, Khlopina 8/3, 194021 St.-Petersburg, Russia

V. G. Dubrovskii (✉) · G. E. Cirlin
Ioffe Physical-Technical Institute RAS, Politekhnicheskaya 26, 194021, St.-Petersburg, Russia
e-mail: dubrovskii@mail.ioffe.ru

G. E. Cirlin · C. Sartel · J. C. Harmand · F. Glas
CNRS-LPN, Route de Nozay, 91460 Marcoussis, France

M. Tchernycheva
Department OptoGaN, Institut d'Electronique Fondamentale, UMR 8622 CNRS, 91405 Orsay Cedex, France

Introduction

A rapidly growing interest in self-standing NWs of III–V compound semiconductors is explained by an interesting physics of their growth [1–6], crystal structure [6, 7] transport [8] and optical [9] phenomena as well as a variety of promising applications in nanoelectronics [8] and nanophotonics [9, 10]. III–V NWs with radii of the order of 10 nm and length up to ten micrometers are usually fabricated by metal organic chemical vapor deposition (MOCVD) [1, 2] or MBE [3–7] via the so-called vapor–liquid–solid (VLS) mechanism [11] on the substrates activated by a metal (Au) growth catalyst. Due to their ability to accommodate strain in two dimensions, NWs are ideal candidates for monolithic integration of dissimilar semiconductor materials, e.g., of III–V compounds on Si [12, 13]. For the controlled production of NWs with the desired morphology and crystal structure, it is important to understand major kinetic processes driving NW growth at given set of deposition conditions. Furthermore, theoretical and experimental investigations into NW formation mechanisms can provide important information on many kinetic characteristics (e.g., supersaturations, diffusion lengths and surface energies [1–5, 14–22]) that are otherwise not easy to measure or even define theoretically.

Since the dominant growth direction of NWs is ⟨111⟩, most growth experiments [1–6] are carried out on the (111) oriented surfaces, with NWs being perpendicular to the substrate. As regards the growth mechanisms of such NWs, semiconductor material is transferred to the drop (seated at the NW top) by different kinetic pathways: the direct

impingement onto the drop surface and the surface diffusion of adatoms that first impinge the sidewalls and substrate [1–6, 14–22]. The diffusion-induced contribution into the overall growth rate is always dominant in MBE [3–6, 14, 22]. For very thin NWs, it is important to consider the Gibbs–Thomson (GT) effect of elevation of chemical potential caused by the curvature of the drop surface [2, 15]. In MBE case, the flux directly impinging the sidewalls increases with the incident angle of the beam. The use of substrate orientation other than (111), resulting in the formation of inclined NWs with varying tilt angle (and consequently the incident angle of the beam), can therefore provide an additional parameter to alter the NW morphology. The incident angle of the flux impinging the tilted NW is, however, changing in time if the substrate is rotating, so a proper averaging should be introduced to generalize the existing models. The use of high-index substrates, implemented earlier, e.g., for the growth of InGaAs/GaAs quantum wells [23], can be of particular importance in connection with the phase perfection: as demonstrated in Refs. [7, 24], the use of particular high-index GaAs substrates for the Au-seeded MBE growth of GaAs NWs produces stacking fault-free zincblende structure.

In this work, we report on theoretical and experimental investigation into the Au-assisted MBE of inclined GaAs NWs. A theoretical model of Refs. [6, 15] is developed to describe the growth of inclined NWs and to find explicitly the dependence of NW growth rate as a function of tilt angle at given set of deposition conditions. We then carry out MBE growth experiments on the GaAs(211)A and GaAs(111)B substrates. From the analysis of scanning electron microscopy (SEM) images of different samples, we plot the length-radius curves and fit them by theoretical dependences. This enables to deduce some important kinetic parameters of NW growth, in particular, the effective supersaturations and diffusion lengths on different GaAs surfaces.

Theoretical Model

The model of inclined NW is sketched in Fig. 1. We consider a single NW growing in a stationary mode in z direction making the tilt angle φ to the substrate normal. Neither lateral growth nor shadowing effect is taken into account. The model parameters include the impingement flux J, the incident angle of molecular beam α (in the case of III–V compounds, the growth rate is assumed as being limited by the incorporation of group III element so that α relates to the group III beam), the contact angle of the drop β and the drop surface energy γ. Under the standard assumption of a low concentration of group V element (As)

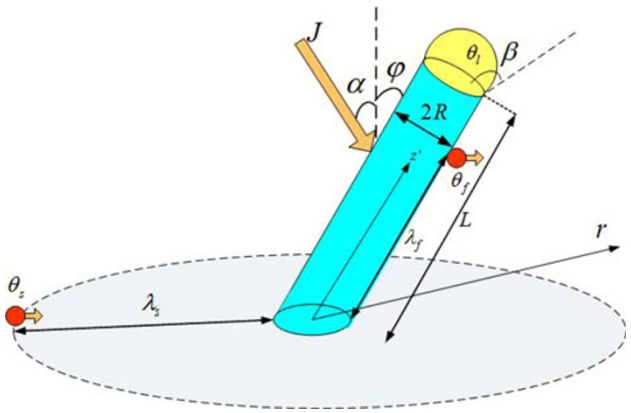

Fig. 1 Illustration of the growth model with the parameters described in the text

in the drop [2, 4, 25], the value of γ must be between the surface energy of pure liquid group III element (Ga) and Au at the growth temperature T. Effective diffusion lengths on the substrate and sidewalls, limited either by desorption or incorporation to a growing surface layer [25], are denoted as λ_s and λ_f, respectively. The quantities θ_v, θ_s, θ_f and θ_l denote the activities (the effective supersaturations) of group III element in the vapor (v), surface adatom (s), sidewall adatom (f) and liquid (l) phases, with the usual definition of $\theta_i = \exp(\mu_i/k_BT)$, where μ_i is the chemical potential in phase i (measured, e.g., with respect to the solid phase) and k_B is the Boltzmann constant [6].

The sidewall impingement rate must be corrected for the effective incident angle of the beam to the inclined NW. Below we consider the general case of rotating substrate, schematized in Fig. 2. The NW growth direction is given by the radius vector $\vec{n} = (\sin\phi\cos\psi, \sin\phi\sin\psi, \cos\phi)$, while the direction of the flux is parallel to the vector $\vec{k} = (0, \sin\alpha, \cos\alpha)$. For the incident angle of the beam to the NW ξ, this yields:

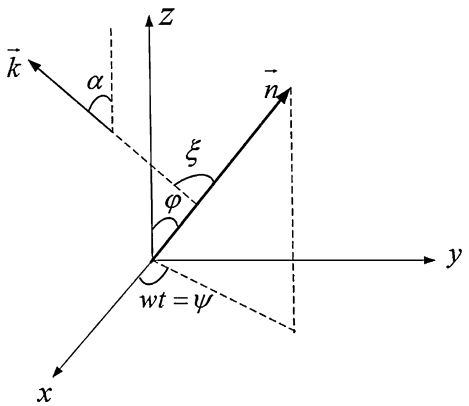

Fig. 2 Direction $\vec{k}$ parallel to the flux and the momentum growth direction of NW $\vec{n}$ at time t (with respect to stationary coordinates x and y) defined by the tilt angle ϕ and the angle $\psi = \omega t$, with ω as the angular velocity of substrate rotation

$$\cos\xi = \sin\alpha\sin\varphi\sin\psi + \cos\alpha\cos\varphi. \quad (1)$$

The activities of adatom phases [6, 15] can be now put in the form

$$\theta_s = J\tau_s\sigma_s\cos\alpha; \quad \theta_f = J\tau_f\sigma_f\langle\sin\xi\rangle. \quad (2)$$

Here, σ_s, σ_f are the elementary areas of substrate and sidewall surfaces, and τ_s, τ_f are the corresponding adatom lifetimes. The quantity $\langle\sin\xi\rangle$ denotes the mean value of $\sin\xi$ averaged over the substrate revolution. Obviously,

$$\langle\sin\xi\rangle = \frac{1}{2\pi}\int_0^{2\pi} d\xi\sqrt{1-\cos^2\xi}, \quad (3)$$

where $\cos\xi$ is given by Eq. 1. Our numerical analysis shows that Eq. 3 can be well approximated (with less than 7% error) by the simplified formula $\langle\sin\xi\rangle \cong \sqrt{1-\langle\cos^2\xi\rangle}$, where, in view of Eq. 1, $\langle\cos^2\xi\rangle = \cos^2\alpha\cos^2\varphi + (1/2)\sin^2\alpha\sin^2\varphi$. With this approximation, we get

$$\langle\sin\xi\rangle \cong \sqrt{1-\cos^2\alpha\cos^2\varphi - \frac{1}{2}\sin^2\alpha\sin^2\varphi}, \quad (4)$$

the expression used hereinafter for the effective incident angle to the inclined NWs. Obviously, Eq. 4 [as well as general Eqs. 1 and 3] is reduced to trivial identity $\langle\sin\xi\rangle = \sin\alpha$ at $\varphi = 0$, i.e., the growth of straight NWs is not influenced by the substrate rotation.

The detailed analysis of Refs. [6, 15] shows that the exact solution for the stationary NW growth rate has the form

$$\frac{dL}{dH} = A + \frac{BU(L/\lambda_f) + C}{U'(L/\lambda_f)}. \quad (5)$$

Here, L is the NW length, $H = Vt$ is the effective deposition thickness at time t, $V = J\Omega_s\cos\alpha$ is the deposition rate (with Ω_s as the elementary volume in the solid phase) and $\lambda_f = \sqrt{D_f\tau_f}$ is the effective diffusion length on the sidewalls (with D_f as the corresponding diffusion coefficient). The A term describes the direct impingement onto the drop surface [26], the desorption from the drop and the growth of surface layer. Since in our experiments the inequality $\beta > \pi/2 + \xi$ [26] holds for most ξ during the substrate rotation, the corresponding averaging is almost independent on the incident angle ξ:

$$A = \frac{1}{\cos\alpha\sin^2\beta}\left[1 - 2(1-\cos\beta)\frac{\exp(R_{GT}/R)}{\theta_{vl}}\right] - \varepsilon. \quad (6)$$

The desorption term contains the standard GT modification of liquid activity θ_l [2, 6], with $R_{GT} = (2\gamma\Omega_l\sin\beta)/(k_BT)$ as the characteristic GT radius and Ω_l as the elementary liquid volume. The desorption rate is inversely proportional to the ratio of activities in the vapor and infinitely large liquid alloy, $\theta_{vl} \equiv \theta_v/\theta_l^\infty$. The quantity $\varepsilon = V_s/V$ accounts for the substrate growth, with V_s as the growth rate on the non-activated surface [3].

The second, L-dependent term in the right hand side of Eq. 5 gives two diffusion-induced contributions, one originating from the adatoms impinging the sidewalls and migrating to the drop and another caused by the adatoms that first impinge the substrate and then diffuse to the drop along the sidewalls. The coefficients B (describing the sidewall adatoms) and C (describing the substrate adatoms) in the case of MBE are given by [6]

$$B = \frac{2\lambda_f\langle\sin\xi\rangle}{\pi R\cos\alpha}\left[1 - \frac{\exp(R_{GT}/R)}{\theta_{fl}}\right];$$
$$C = \frac{2\lambda_s}{R}\delta(R/\lambda_s)\left[1 - \frac{\exp(R_{GT}/R)}{\theta_{sl}}\right]. \quad (7)$$

Here, $\theta_{fl} \equiv \theta_f/\theta_l^\infty$ and $\theta_{sl} \equiv \theta_s/\theta_l^\infty$ are the effective supersaturations of sidewall and surface adatoms with respect to the infinite liquid alloy, $\delta(R/\lambda_s) = K_1(R/\lambda_s)/K_0(R/\lambda_s)$, $\lambda_s = \sqrt{D_s\tau_s}$ is the effective diffusion length on the substrate surface (with D_s as the corresponding diffusion coefficient) and $K_n(x)$ are the modified Bessel function of the second kind of order n. Further, the functions $U(L/\lambda_f)$ and $U'(L/\lambda_f)$ in Eq. 5 are defined as follows

$$U(L/\lambda_f) = \sinh(L/\lambda_f) + \nu\delta(R/\lambda_s)\left[\cosh(L/\lambda_f) - 1\right];$$
$$U'(L/\lambda_f) \equiv dU/d(L/\lambda_f) = \cosh(L/\lambda_f) + \nu\delta(R/\lambda_s)\sinh(L/\lambda_f) \quad (8)$$

with

$$\nu \equiv \frac{D_s\sigma_f\lambda_f}{D_f\sigma_s\lambda_s} = \frac{\pi\lambda_s}{\lambda_f}\frac{\theta_{fl}}{\theta_{sl}}\frac{\cos\alpha}{\langle\sin\xi\rangle}. \quad (9)$$

At given MBE growth conditions (T, V, α, V/III fluxes ratio), the vapor–solid chemical potential and consequently the vapor supersaturation is well defined [25], but it generally tells nothing about the quantity θ_{vl} entering Eq. 6 for A. If, however, the growth temperature is low enough, we can safely neglect the desorption term in Eq. 6 (perhaps excluding very thin NWs) and eliminate unknown θ_{vl}. In this case, with the known material constants (providing the GT radius R_{GT}), contact angle β and tilt angle ϕ, the measured $L(H)$ or $L(R)$ curves of inclined NWs can be fitted by four parameters, two diffusion lengths λ_s, λ_f and two supersaturations θ_{fl}, θ_{sl}. At $L/\lambda_f \ll 1$ and $\lambda_s/\lambda_f \ll 1$, the dependence on λ_f disappears. The non-vanishing terms at $L/\lambda_f \to 0$ and $\lambda_s/\lambda_f \to 0$ (yielding also $\tau_s/\tau_f \to 0$) reduce Eqs. 5, 8, 9 to the non-linear growth equation of the form [27]

$$\frac{dL}{dH} = \frac{a_0 + a_1L/\lambda_s + a_2(L/\lambda_s)^2}{1 + b\delta(R/\lambda_s)L/\lambda_s} \quad (10)$$

with coefficients

$$a_0 = A + C; \quad a_1 = Ab\delta(R/\lambda_s) + (\lambda_s/\lambda_f)B;$$
$$a_2 = (\lambda_s/2\lambda_f)Bb\delta(R/\lambda_s); \quad b = \frac{D_s\sigma_f}{D_f\sigma_s}. \tag{11}$$

Thus, our model provides the exact solution for the NW growth rate with the tilt angle as the control parameter. This solution contains, however, a number of unidentified quantities that can be found only from the direct comparison with experiment.

Growth Experiments

Our growth experiments were carried out with a Riber 32 MBE setup equipped with solid sources supplying monomers of Ga and tetramers of As_4. Growth was performed on the GaAs (111)B and GaAs(211)A substrates. During the growth, the substrates rotation was applied. Incident angle of Ga flux α amounted to 16.7° to the normal. Substrate surfaces were deoxidized at 620°C, and a 30 nm GaAs buffer layers were grown to achieve atomically flat surface. Then, the substrate temperature was decreased and stabilized to $T = 550$°C for the NW growth on the both types of substrates. For catalyst deposition, Au source installed directly into the growth chamber in a regular effusion cell was used. This configuration enables to deposit the catalyst on chemically clean surface, and at the same time to control the substrate temperature and monitor the deposition process with reflection high-energy electron diffraction. An amount of Au equivalent to a uniform layer of ~ 1 nm was deposited on the substrate surface to promote the NW growth. This procedure resulted in the formation of Au droplets alloyed with the substrate constituents which could activate the NW growth. Since the growth temperature of 550°C is much higher than the lowest eutectic temperatures of Au–Ga alloy (339.4°C and 348.9°C [28]), the drop must remain liquid during the growth. For all samples, the nominal growth rate V was fixed to 0.2 nm/s, the V/III flux ratio was equal 3 and the effective deposition thickness was fixed to 360 nm with the corresponding deposition time of 30 min.

The morphology of as-grown GaAs NW ensembles was investigated using field-emission SEM technique. Figures 3 and 4 present typical SEM images of GaAs NWs grown on the GaAs(111)B and GaAs(211)A substrates, respectively, under identical deposition conditions described hereinabove. It is seen that all NWs have almost uniform radius from base to top, which agrees with the results of Ref. [29] where the pronounced lateral growth [18, 19] was observed only below 500°C. This justifies the assumption of NW elongation at $R = \text{const}$. As expected, the NWs grown on the (111)B substrate are perpendicular to the surface. From the analysis of plan and top view SEM images, the tilt angle of NWs on the (211)A substrate varies from 15 to 30°, with the statistical average around 20°, which equals the angle between the (211) plane and ⟨111⟩ crystallographic direction. This confirms the dominant ⟨111⟩ growth direction of inclined NWs. The measured lengths of selected NWs and the average thickness of surface layer on the non-activated substrates are shown in the figures. Statistical analysis of SEM images presented in Figs. 3 and 4 enables to plot out the length-radius dependences shown by points in Fig. 5.

Results and Discussion

From Fig. 5, the length of all NWs is noticeably larger than the deposition thickness (360 nm), and is almost 6 times

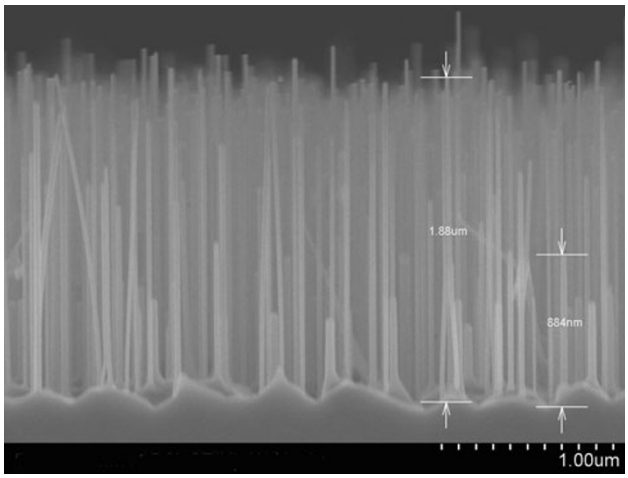

Fig. 3 Cross-view SEM image of straight GaAs NWs on the GaAs(111)B substrate

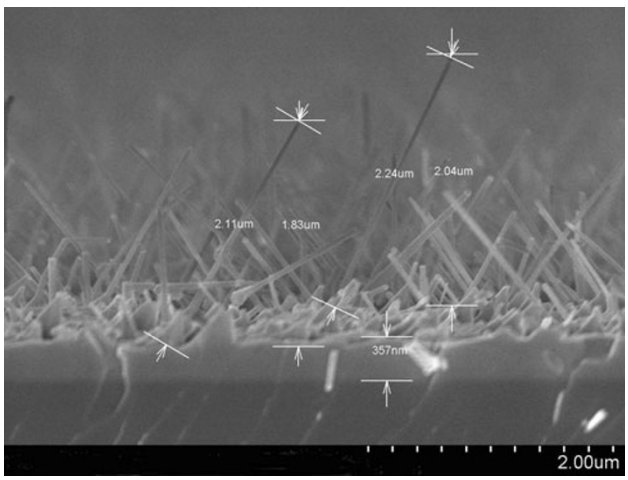

Fig. 4 Cross-view SEM image of inclined GaAs NWs on the GaAs(211)A substrate. Average tilt angle equals 20°, average thickness of surface layer is 357 nm, with the initial buffer layer thickness of 30 nm

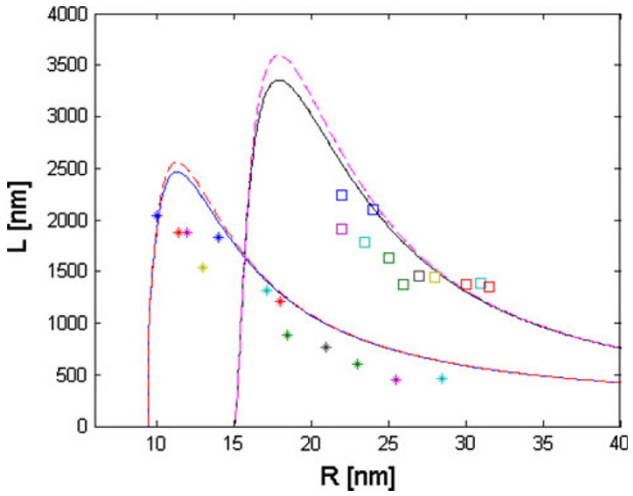

Fig. 5 Experimental (*points*) and theoretical (*lines*) length-radius dependences of straight (*stars*) and inclined (*open squares*) GaAs NWs. Fits are obtained from exact Eqs. 5–9 [*solid lines*] and simplified Eqs. 10 and 11 [*dotted lines*] with the parameters summarized in Table 1

larger for longest 2 μm NWs, which proves the diffusion-induced character of NW growth discussed previously in Ref. [1–6, 14–22]. The solid lines in Fig. 5 are obtained from general expressions given by Eqs. 2, 4, 5–9 with the parameters summarized in Table 1. The dotted lines correspond to simplified Eqs. 10 and 11 with the same fitting parameters. According to the data of Ref. [25], the vapor supersaturation $\theta_v = \exp(\Delta\mu_v/k_BT)$ with respect to the GaAs(111)B substrate equals approximately 183 at $T = 550$°C,, so that the assumption of $\theta_{vl} \to \infty$ (i.e., negligible re-evaporation from the drop) looks reasonable. At $T = 550$°C, the average contact angle of the drops $\beta = 120°$ and $\gamma = 1.0$ J/m^2 (corresponding to approximately 40% Ga concentration in the liquid Au–Ga alloy during the growth [15]), the GT radius R_{GT} equals 5.8 nm. With neglect of desorption, the value of ε in Eq. 6 is estimated as $\varepsilon \cong H_s/H = 327/360 = 0.91$, i.e. only 9% of material is distributed in the NWs and 91% remains in a 2D surface layer growing concomitantly with the NWs. As follows from Fig. 5, the simplified growth equation at $L/\lambda_f \to 0$ is a good approximation to the general expressions for the parameters considered. A small difference which can be seen for the longest NWs with $L > 2$ μm is explained by the re-evaporation of some Ga adatoms from the sidewalls. Due to this desorption, the actual length becomes smaller than that predicted by the simplified formula where the re-evaporation is neglected. As in Refs. [2, 15, 25], theoretical model predicts the non-monotonous behavior of the $L(R)$ curves, reaching their maxima due to the balance of the GT and the diffusion-induced contributions into the overall growth rate. The GT effect suppresses completely the growth of straight GaAs with $R < 9$ nm and inclined GaAs NWs with $R < 15$ nm. The obtained estimate of minimum radius for the straight GaAs NWs is consistent with the result of Ref. [2] in the case of Au-catalyzed MOCVD of straight InAs NWs ($\sim$8 nm at $T = 425$°C).

As follows from the results summarized in Table 1, the effective diffusion length on the substrate surfaces (limited by the incorporation into a growing surface layer) appears to be only 12 nm for the both substrates studied. This estimate is noticeably smaller than the previously obtained results of 25 nm (Ref. [22]) and 35 nm (Ref. [14]) at 560°C. Such difference is most probably explained by the simplified growth equation used in Ref. [14, 22], i.e., $dL/dH = a_0$ instead of Eq. 10, resulting in the neglect of sidewall adatoms. It is noteworthy that the non-linear terms in L/λ_s in Eqs. 10, 11 contain the contributions from sidewall adatoms through the λ_f-independent coefficients $(\lambda_s/\lambda_f)B$ in the corresponding Eqs. 11 for a_1 and a_2. These contributions cancel exactly only at $B = 0$, i.e., for straight NWs ($\phi = 0$) and the beam being strictly perpendicular to the substrate ($\alpha = 0$). Otherwise, the diffusion of adatoms directly impinging the NW sidewalls plays an important role even at the initial stage of NW growth with $L/\lambda_f \ll 1$, the effect overlooked in the number of recent studies [2, 14, 22]. Since our NWs are relatively short, the fit obtained from general expressions given by Eqs. 5–9 becomes independent on λ_f at $\lambda_f \geq 5{,}000$ nm. We can therefore conclude that the effective diffusion length of Ga atoms on the NW sidewalls (which should be constructed from six equivalent $(2\bar{1}\bar{1})$ facets in the case of zincblende NWs or their $(1\bar{1}00)$ wurtzite counterparts [25]) is more than 5,000 nm. This result is consistent with previous estimates, e.g., 3,000 nm at 590°C in Ref. [4].

As regards the obtained estimates for the effective supersaturations, the first obvious conclusion is that the inequalities $\theta_{sl} > 1$ and $\theta_{fl} > 1$ yield positive (i.e., directed from base to top) diffusion fluxes at $R_{GT}/R \ll 1$ for the surface and sidewall adatoms, because the adatom chemical potentials are larger than the chemical potential of infinite liquid alloy [6]. The corresponding flux becomes negative only for sufficiently thin NWs due to the GT effect. For the both cases considered, the supersaturation of sidewall

Table 1 Growth conditions and fitting parameters for different GaAs NWs

Substrate	T (°C)	ϕ (deg)	λ_s (nm)	θ_{sl}	$\Delta\mu_{sl}$ (meV)	λ_f (nm)	θ_{fl}	$\Delta\mu_{fl}$ (meV)
GaAs(111)B	550	0	12	1.67	36.5	5,000	11.2	172
GaAs(211)A	550	20	12	1.40	24.0	5,000	16.3	199

adatoms is several times larger than that of surface adatoms, which is qualitatively consistent with the strong inequality $\lambda_f/\lambda_s \gg 1$. The supersaturation of sidewall adatoms is noticeably larger for the inclined NWs (16.3 against 11.2 for the straight NWs), which is again explained by a larger impingement onto the tilted sidewalls. The corresponding differences in chemical potentials in the adatom and infinite liquid phases, obtained from the relationships $\theta_{sl} = \exp(\Delta\mu_{sl}/k_BT)$; $\theta_{fl} = \exp(\Delta\mu_{fl}/k_BT)$, equal 24.0–36.5 meV for the surface and 172–199 meV for the sidewall adatoms.

To sum up, our results show that the diffusion of adatoms that first impinge the sidewalls has a tremendous effect on the growth rate. First, since the diffusivity of surface adatoms during MBE is fundamentally limited by the growing surface layer, and their supersaturation is much lower than that of the sidewall adatoms, the coefficient C in Eq. 5 is usually much smaller than B and even much smaller than A. Therefore, the initial growth stage should be controlled by the direct impingement onto the drop surface (A), while the contribution from the sidewall adatoms (B) rapidly increases as the NW elongates. Second, our experimental data and theoretical fits demonstrate that the inclined $\langle 111 \rangle$ NWs grow much faster than the straight ones: from Fig. 4, the GaAs NWs on the GaAs(211)A substrate are more than 2 times larger at the same radii and otherwise identical deposition conditions. Better analysis could be performed with the experimental length–time dependences, where different contributions at different growth stages would be more easily distinguished [30, 31]. As yet, however, we do not have in hand such experimental data for the inclined GaAs NWs. As the NWs grow, the shadowing effect might become important at a certain critical length which can be easily estimated with given incident angle of the beam and the NW density. We now plan to consider these effects from the viewpoint of the obtained results.

Acknowledgments This work was partially supported by the 111 Project (No. B07005), Program for Changjiang Scholars and Innovative Research Team in University (No. IRT0609), National Basic Research Program of China (No. 2010CB327600), Russian Federal Agency for Science and Innovation (Contract No. 02.740.11.0383), the scientific program of Russian Academy of Sciences "Fundamental aspects of nanotechnologies and nanomaterials" and few grants of Russian Foundation for Basic Research.

References

1. W. Seifert, M. Borgstrom, K. Deppert, K.A. Dick, J. Johansson, M.W. Larsson, T. Martensson, N. Skold, C.P.T. Svensson, B.A. Wacaser, L.R. Wallenberg, L. Samuelson, J. Cryst. Growth **272**, 211 (2004)
2. L.E. Fröberg, W. Seifert, J. Johansson, Phys. Rev. B **76**, 153401 (2007)
3. V.G. Dubrovskii, G.E. Cirlin, I.P. Soshnikov, A.A. Tonkikh, N.V. Sibirev, Yu.B. Samsonenko, V.M. Ustinov, Phys. Rev. B **71**, 205325 (2005)
4. J.C. Harmand, G. Patriarche, N. Péré-Laperne, M.-N. Mérat-Combes, L. Travers, F. Glas, Appl. Phys. Lett. **87**, 203101 (2005)
5. M.C. Plante, R.R. LaPierre, J. Cryst. Growth **286**, 394 (2006)
6. V.G. Dubrovskii, N.V. Sibirev, G.E. Cirlin, A.D. Bouravleuv, Yu.B. Samsonenko, D.L. Dheeraj, H.L. Zhou, C. Sartel, J.C. Harmand, G. Patriarche, F. Glas, Phys. Rev. B **80**, 066940 (2009)
7. H. Shtrikman, R. Popovitz-Biro, A. Kretinin, M. Heiblum, Nano Lett. **9**, 215 (2009)
8. M.T. Bjork, B.J. Ohlsson, T. Sass, A.I. Persson, C. Thelander, M.H. Magnusson, K. Deppert, L.R. Wallenberg, L. Samuelson, Appl. Phys. Lett. **80**, 1058 (2002)
9. J. Xiang, W. Lu, Y.J. Hu, Y. Wu, H. Yan, C.M. Lieber, Nature **441**, 489 (2006)
10. G.E. Cirlin, A.D. Bouravleuv, I.P. Soshnikov, Yu.B. Samsonenko, V.G. Dubrovskii, E.M. Arakcheeva, E.M. Tanklevskaya, P. Werner, Nanoscale Res. Lett. **5**, 360 (2010)
11. R.S. Wagner, W.C. Ellis, Appl. Phys. Lett. **4**, 89 (1964)
12. L.C. Chuang, M. Moewe, S. Crankshaw, C. Chase, N.P. Kobayashi, C. Chang-Hasnain, Appl. Phys. Lett. **90**, 043115 (2007)
13. G.E. Cirlin, V.G. Dubrovskii, I.P. Soshnikov, N.V. Sibirev, Yu.B. Samsonenko, A.D. Bouravleuv, J.C. Harmand, F. Glas, Phys. Stat. Sol. RRL **3**, 112 (2009)
14. V.G. Dubrovskii, N.V. Sibirev, R.A. Suris, G.E. Cirlin, J.C. Harmand, V.M. Ustinov, Surf. Sci. **601**, 4395 (2007)
15. V.G. Dubrovskii, N.V. Sibirev, G.E. Cirlin, I.P. Soshnikov, W.H. Chen, R. Larde, E. Cadel, P. Pareige, T. Xu, B. Grandidier, J.-P. Nys, D. Stievenard, M. Moewe, L.C. Chuang, C. Chang-Hasnain, Phys. Rev. B **79**, 205316 (2009)
16. J. Johansson, C.P.T. Svensson, T. Martensson, L. Samuelson, W. Seifert, J. Phys. Chem. B **109**, 13567 (2005)
17. I. Avramov, Nanoscale Res. Lett. **2**, 235 (2007)
18. M.C. Plante, R.R. LaPierre, J. Appl. Phys. **105**, 114304 (2009)
19. V.G. Dubrovskii, N.V. Sibirev, G.E. Cirlin, M. Tchernycheva, J.C. Harmand, V.M. Ustinov, Phys. Rev. E **77**, 031606 (2008)
20. S.N. Mohammad, J. Vac. Sci. Technol. **28**, 329 (2010)
21. E. De Jong, R.R. LaPierre, J.Z. Wen, Nanotechnology **21**, 045602 (2010)
22. V.G. Dubrovskii, N.V. Sibirev, R.A. Suris, G.E. Cirlin, V.M. Ustinov, M. Tchernysheva, J.C. Harmand, Semiconductors **40**, 1075 (2006)
23. Z. Li, J. Wu, Z.M. Wang, D. Fan, A. Guo, S. Li, S.-Q. Yu, O. Manasreh, G.J. Salamo, Nanoscale Res. Lett. **5**, 1079 (2010)
24. H. Shtrikman, R. Popovitz-Biro, A. Kretinin, L. Houben, M. Heiblum, M. Bukala, M. Galicka, R. Buczko, P. Kacman, Nano Lett. **9**, 1506 (2009)
25. V.G. Dubrovskii, N.V. Sibirev, J.C. Harmand, F. Glas, Phys. Rev. B **78**, 235301 (2008)
26. F. Glas, Phys. Stat. Sol. B **247**, 254 (2010)
27. V.G. Dubrovskii, N.V. Sibirev, M.A. Timofeeva, Semiconductors **43**, 1226 (2009)
28. T.B. Massalski (ed.), *Binary alloy phase diagrams*, vol. 1, 1st edn. (American Society for Metals, Metals Park, OH, 1986), p. 260
29. J.C. Harmand, M. Tchernycheva, G. Patriarche, L. Travers, F. Glas, G. Cirlin, J. Cryst. Growth **301–302**, 853 (2007)
30. M. Tchernycheva, L. Travers, G. Patriarche, F. Glas, J.C. Harmand, G.E. Cirlin, V.G. Dubrovskii, J. Appl. Phys. **102**, 094313 (2007)
31. F. Glas, J.C. Harmand, G. Patriarche, Phys. Rev. Lett. **104**, 135501 (2010)